Received: 9 August 2023 | Revised: 5 October 2023 | Accepted: 31 October 2023

DOI: 10.1111/pce.14764

ORIGINAL ARTICLE

Plant, Cell & Environment | WILEY

Plasticity in branch water relations and stem hydraulic vulnerability enhances hydraulic safety in mangroves growing along a salinity gradient

Holly A. A. Beckett[1] | Callum Bryant[1] | Teresa Neeman[2] | Maurizio Mencuccini[3] | Marilyn C. Ball[1]

[1]Plant Science Division, Research School of Biology, Australian National University, Canberra, Australia

[2]Biological Data Science Institute, Australian National University, Canberra, Australia

[3]Ecological and Forestry Applications Research Centre (CREAF), Barcelona, Bellaterra, Spain

Correspondence
Holly A. A. Beckett, Plant Science Division, Research School of Biology, Australian National University, Canberra, ACT 2601, Australia.
Email: Holly.beckett@anu.edu.au

Funding information
Australian Government Research Training Program; Australian Research Council

Abstract

Coping with water stress depends on maintaining cellular function and hydraulic conductance. Yet measurements of vulnerability to drought and salinity do not often focus on capacitance in branch organs that buffer hydraulic function during water stress. The relationships between branch water relations, stem hydraulic vulnerability and stem anatomy were investigated in two co-occurring mangroves *Aegiceras corniculatum* and *Rhizophora stylosa* growing at low and high salinity. The dynamics of branch water release acted to conserve water content in the stem at the expense of the foliage during extended drying. Hydraulic redistribution from the foliage to the stem increased stem relative water content by up to 21%. The water potentials at which 12% and 50% loss of stem hydraulic conductivity occurred decreased by ~1.7 MPa in both species between low and high salinity sites. These coordinated tissue adjustments increased hydraulic safety despite declining turgor safety margins at higher salinity sites. Our results highlight the complex interplay of plasticity in organ-level water relations with hydraulic vulnerability in the maintenance of stem hydraulic function in mangroves distributed along salinity gradients. These results emphasise the importance of combining water relations and hydraulic vulnerability parameters to understand vulnerability to water stress across the whole plant.

KEYWORDS
capacitance, hydraulic redistribution, hydraulic safety margin, plant segmentation, salinity tolerance, turgor safety margin, water storage

1 | INTRODUCTION

Anthropogenic climate change has already resulted in ecosystem collapse and community composition shifts due to a global increase in extreme weather events, drought, and changes in rainfall distribution (IPCC, 2022). In the case of mangroves, as the incidence of such extreme weather events increase, large-scale die back is predicted to increase with severe consequences for the ecosystems, industries and communities that rely on these forests (Duke et al., 2017; Harris et al., 2018; Oliveira et al., 2014). Thus, there is an urgent need to understand how morphological and physiological traits interact to enhance drought and salinity tolerance.

Hydraulic failure is widely considered the predominant mechanism for drought (Adams et al., 2017) and salinity (McDowell et al., 2022a) induced mortality under extreme conditions. However, plants may manage hydraulic risk via plastic adjustment of water within the plant. For example, water storage and hydraulic capacitance, two important water relations parameters, can reduce hydraulic vulnerability in mangroves when salinity or drought conditions increase (Bryant et al., 2021; Coopman et al., 2021). Understanding the plasticity of traits that contribute to buffering hydraulic function under varied growth conditions is critical to understanding species' resilience to drought and increased salinity (Guadagno et al., 2017; McDowell et al., 2022b), yet remains poorly resolved.

Water storage (WS, the volume of water released from storage tissues), and capacitance (*C*, the amount of water released for a given change in water potential) (Oliva Carrasco et al., 2015; Scholz et al., 2011), play essential roles in the water balance of trees, contributing 10%–50% of total daily transpiration depending on the species (Goldstein et al., 1998; Holbrook & Sinclair, 1992; Loustau et al., 1996; Scholz et al., 2007; Steppe & Lemeur, 2004; Waring et al., 2006). The capacitive release of stored water buffers xylem tissue from greater changes in water potential (ψ) and tension that can cause lethal embolism during drought (Bryant et al., 2021; Coopman et al., 2021; Meinzer et al., 2003, 2008; Preisler et al., 2022), and can play a pivotal role in enabling maintenance of high rates of water use during rapid growth, and embolism repair (Brodersen et al., 2010; Nardini et al., 2011; Robert et al., 2009; Salleo et al., 2009; Sevanto et al., 2014). For example, Nguyen et al. (2017b) found release of water from leaf storage tissues could sustain transpiration rates for up to 2 h.

WS and *C* are measured from water release curves (Δwater content/$\Delta\psi$) (Cheung et al., 1975; Nguyen et al., 2017b; Scholander et al., 1964; Tyree & Hammel, 1972). Water release curves have been well studied in leaves (Bartlett et al., 2012), but few studies have focused on canopy branch water release (branch = foliage and attached stem in the canopy) to understand the relative contributions that foliage and stem organs make to the maintenance of whole branch function during drying (Bryant et al., 2021; Gleason et al., 2014; Martinez-Vilalta et al., 2019). Shifting availability of water within and between foliage and stem organs across early and late dry season has been shown to enable the mangrove *Sonneratia alba* to mitigate the loss of hydraulic conductance, despite no change in key measures of hydraulic vulnerability (Bryant et al., 2021). In this way, hydraulic segmentation between stems and foliage may enable release of water from foliage tissues that preserves stem hydraulic function during drought (Hochberg et al., 2016; Rodriguez-Dominguez et al., 2018; Zimmermann, 1983).

The living tissues of the stem (inner bark, cortex and ray parenchyma, Figure 1) are thought to make up the majority of stem WS. This is because these cell types have more elastic walls than those of lignified xylem fibres and conduits, allowing for greater changes in volume for a given change in ψ (Pfautsch et al., 2015). Therefore, stem *C* and WS are hypothesised to correlate with the proportion of living cells due to the need to mobilise significant volumes of stored water quickly to avoid the hazardous development of large ψ gradients (Meinzer et al., 2009; Pfautsch et al., 2015). Indeed, studies of angiosperms have found ray tissue in the xylem can account for 40% of the sapwood volume (Panshin & De Zeeuw, 1980) and up to 75% in species with high *C* and WS (Chapotin et al., 2006). In addition, dye injection experiments have shown that radial water transport occurs primarily through ray parenchyma facilitating water transport from storage into xylem (Pfautsch et al., 2015). Interspecific variation in the structure of tissues involved in *C* and WS, and *C* and WS plasticity between organs interact with maintenance of hydraulic function and turgor. Thus, improving resolution of *C* and WS function is central to understanding species differences in vulnerability to extremes in drought and salinity.

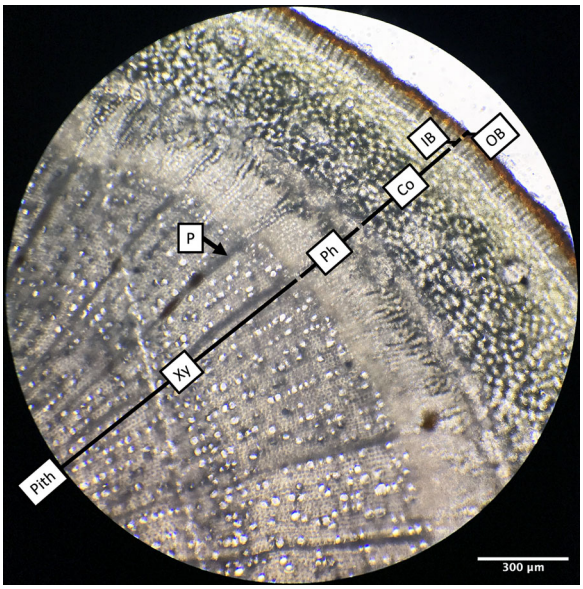

FIGURE 1 Transverse section illustrating tissue layers of a stem section of *Aegiceras corniculatum* collected from a high salinity site on the Daintree River. Co, cortex; IB, inner bark; OB, outer bark; P, parenchyma; Ph, phloem; Xy, xylem.

The ψ corresponding with the air entry threshold at 12% loss of hydraulic conductivity (P12), and the threshold for xylem failure at 50% loss of hydraulic conductivity (P50, Arend et al., 2021; Domec & Gartner, 2001; Mantova et al., 2022; Martin-StPaul et al., 2017; Meinzer et al., 2009; Trueba et al., 2017), are used as indicators of a plant's vulnerability to stem hydraulic failure during dehydration. Similarly, the leaf turgor loss point (ψ_{TLP}) can be used to indicate interspecific and intraspecific variation in the vulnerability of living plant tissues to dehydration due to drought (Bartlett et al., 2012; Bryant et al., 2021) and salinity (Naidoo et al., 2011; Naidoo, 1985; Nguyen et al., 2017a). Turgor is essential for cellular function, growth, communication, and transport (Fricke, 2017; Peters et al., 2021). When dehydration causes loss of turgor, further dehydration impairs cellular function and can eventually result in cell death if hydration is not recovered (Lambers & Oliveira, 2019). Therefore, ψ_{TLP} represents the critical point below which turgor-dependent plant function is impaired.

Within and across biomes and among species, P12, P50, and ψ_{TLP} have been shown to vary with water availability (Bartlett et al., 2012; Bartlett et al., 2016; Choat et al., 2012). However, while mangroves

adjust ψ_{TLP} in response to increases in salinity (Naidoo et al., 2011; Naidoo, 1985) and seasonal drought (Bryant et al., 2021), few studies have investigated plasticity in stem hydraulic vulnerability in mangrove species tolerant of a wide range of salinities. Limited capacity for adjustment of hydraulic vulnerability would leave a mangrove species growing along an environmental gradient vulnerable to the extremes in its environment. Thus, while the plasticity of hydraulic vulnerability traits within species is central to predicting survival, it remains poorly understood in mangroves.

Mangrove species distributed along a salinity gradient provide an ideal study system to explore the influence of the ψ of estuarine water at the roots ($\psi_{estuary}$) on the plasticity of traits in response to water scarcity. Because plants must maintain lower ψ in their roots than that of $\psi_{estuary}$ to enable passive water uptake (Scholander et al., 1964), the $\psi_{estuary}$ determines the degree of hydration achievable through the roots (Scholander et al., 1964). Therefore, the difference between $\psi_{estuary}$, and ψ_{TLP} in leaves defines the turgor safety margin (TSM); the range of ψ over which the plant can operate while maintaining turgor from root water. In the mangroves *Aegiceras corniculatum* and *Rhizophora stylosa*, Beckett et al. (2023) found that despite lowering ψ_{TLP} in response to increasing salinity, plasticity in ψ_{TLP} was less than proportionate with the increase in $\psi_{estuary}$, reducing the TSM with increasing salinity. Because of the importance of turgor for growth and carbon gain (Fricke, 2017; Peters et al., 2021), reduction in the TSM constrains turgor-dependent function, and increases the risk of cell injury with dehydration below ψ_{TLP}. Similar to the TSM, the hydraulic safety margin (HSM) indicates the range of ψ over which a plant can function before significant loss of hydraulic conductivity occurs (Guillemot et al., 2022). A reduction in the HSM indicates an increased risk of plant hydraulic failure and correlates strongly with greater risk of mortality during drought (Anderegg et al., 2016; Choat et al., 2012; Guillemot et al., 2022; Powers et al., 2020).

There is a high degree of variability in how the HSM has been defined (e.g., Guillemot et al., 2022; Meinzer et al., 2009). However, we suggest here that the margin between $\psi_{estuary}$ and P50 gives the best measure of the range of ψ over which a mangrove can operate while avoiding irrecoverable embolism that could result in plant mortality. Defined this way, a novel comparison between the HSM and the TSM can be made to understand how hydraulic and turgor vulnerability interact to confer drought and salinity tolerance (Table 1).

We aimed to understand how plasticity in branch traits within species maintain turgor and hydraulic safety in mangroves grown at contrasting salinities. Branch water relations, stem hydraulic vulnerability and stem anatomy were measured in two co-occurring mangroves, *Aegiceras corniculatum* (L.) Blanco and *Rhizophora stylosa* Griff., growing at two salinity sites on the Daintree River, Queensland, Australia. These data were used to test the following hypotheses:

H1. The relative contributions of stem WS and *C* to whole-branch water relations decrease with increasing salinity.

H2. Stem *C* increases with the proportions of inner bark, cortex, and ray parenchyma in the stem.

TABLE 1 List of abbreviations.

Parameter	Symbol	Unit
Fresh mass	FM	g
Dry mass	DM	g
Water content	WC	g
Saturated water content per dry mass	WC_{DM}	$g\,g^{-1}$DM
Water potential	ψ	MPa
Water potential of estuarine water at the roots	$\psi_{salinity}$	MPa
Water potential at turgor loss point	ψ_{TLP}	MPa
Relative water content	RWC	%
Water storage (normalised on DM or RWC)	WS	$g\,g^{-1}$DM % RWC_{Branch}
Water storage released before leaf ψ_{TLP}	WS_{TLP}	
Water storage between first and last measurement	WS_{total}	
Water storage capacitance (normalised on DM or RWC)	*C*	$g\,g^{-1}$DM MPa^{-1} % RWC_{Branch} MPa^{-1}
Capacitance before leaf ψ_{TLP}	C_{TLP}	
Capacitance between first and last measurement	C_{total}	
Turgor safety margin	TSM	MPa
Hydraulic safety margin	HSM	MPa
Percent air discharge	PAD	%
Water potential at 50% air discharge	P50	MPa
Water potential at 12% air discharge	P12	MPa

H3. Species improve hydraulic safety when growing at higher salinities by lowering P12 and P50 relative to conspecifics growing at low salinities.

H4. Species' HSMs decrease between low and high salinity sites consistent with declining TSMs with increasing salinity.

2 | MATERIALS AND METHODS

2.1 | Study site and species

Two species that differ in optimum salinities and salt management properties were selected for study: *A. corniculatum*, a salt-secreting species with optimal growth salinities of 10%–20% seawater (Ball, 1988b), and *R. stylosa*, a nonsalt secreting species (Ball, 1988a) with optimal growth salinities of 25%–50% seawater (Clough, 1984).

However, despite *A. corniculatum* being a salt-secretor and *R. stylosa* being a nonsalt secretor, there is no evidence for fundamental differences in bulk water relations between species with different salt management strategies (Beckett et al., 2023). Plant material was collected mid-dry season from trees growing naturally along the banks of the Daintree River, Daintree National Park, Far North Queensland, Australia (16.1700° S, 145.4185° E).

Three estuarine sites (16.257421° S, 145.343296° E; 16.260275 ° S, 145.393811° E; 16.283785° S, 145.451308° E) were selected along the river banks where the geographical position in the estuary and the mangrove vegetation were indicative of different ranges of salinity. Surface water samples were collected at each sampled tree and salinity was measured with a hand-held refractometer (A.S.T. Co. Ltd.). $\psi_{estuary}$ was calculated as a fraction of sea water, where standard seawater has a salinity of 35 parts per thousand (ppt) and a ψ of −2.4 MPa. Along river margins where sediment is loosely consolidated (accreting banks) or where the river banks are well drained and reflooded with successive tides (eroding banks), the surface water salinities are likely to be representative of those used by root systems which were partially exposed to river water, consistent with split root studies of mangroves and other halophytes (Bazihizina et al., 2009, 2012; Reef et al., 2015).

At the time of measurement mid-dry season, estuarine water salinities of 0 ppt (0 MPa) were recorded for the two estuarine sites located up river following heavy rainfall during the wet season and as such these sites were combined as a single 'low salinity' site for analysis. The third site, located near the mouth of the Daintree River, had a salinity of 24 ppt (−1.65 MPa) and is hereafter referred to as the 'high salinity' site.

2.2 | Water relations of branches

Here the branch is defined as the terminal canopy plant growth <1 m in length, composed of a length of stem and its attached leaves. Foliage refers to the collection of individual leaves on the branch, defined to allow differentiation between measurements made on an individual leaf and those on the collection of leaves from the branch. Stem refers to the woody canopy growth to which the leaves are attached.

Canopy branch water-release curves were constructed mid-dry season using a modified bench drying method (Bryant et al., 2021; Gleason et al., 2014). The method is analogous to constructing a pressure-volume (PV) curve for a leaf, but involves integrated responses of a more complex system of tissues and organs. Five trees for each of *A. corniculatum* and *R. stylosa* were selected at high salinity, and 10 trees for *A. corniculatum* and 7 trees for *R. stylosa* were selected at low salinity. One sun-exposed terminal canopy branch <1 m in length was cut from each tree at both sites in the late afternoon, each with several dozen leaves. Branches were transported back to the lab (approximately 30 min) in the dark plastic bags, then were recut under perfusion solution of 1% seawater (~5 mM NaCl) for *R. stylosa* and 5% seawater for *A. corniculatum* and allowed to rehydrate overnight. The composition of the perfusion solution was based on analyses of the ionic composition of xylem sap in *A. corniculatum* and *R. stylosa* grown under lab (Ball, 1988b) and field conditions (Scholander et al., 1966; Stuart et al., 2007).

A water-release curve was constructed and analysed for each individual branch as described by Bryant et al. (2021). Briefly, rehydrated terminal branches were recut above the water line and weighed. Using a Scholander pressure chamber (1050D, PMS Instrument), branch ψ was determined as the average ψ of two leaves, after which branches were reweighed. Branches were then bench dried allowing branch ψ to decline ~0.5 MPa, and incubated in black plastic bags for >40 min to allow equilibration. Decline in fresh mass due to repeated removal of leaves was recorded following each measurement of branch ψ. This sequence was then repeated until completion of the measurements. The dry mass (DM) of each group of leaves incrementally removed during the experiment, plus the remaining attached leaves and stems comprising the branch, were determined after oven drying for 48 h at 70°C to constant mass.

Leaf C and leaf ψ_{TLP} were derived from PV curves constructed using one leaf from each branch as described by Nguyen et al. (2017b). Average leaf C (g g^{-1}DM MPa^{-1}) before and after leaf turgor loss was then used to calculate the change in foliage water fraction of branch WC during drying based on the DM of leaves on the branch and $\Delta\psi$ at each measurement. Foliage WC was then subtracted from total branch WC to determine the remaining stem WC.

C changes with branch ψ over the total water release curve. Therefore, C can be estimated over different ranges of ψ (Bartlett et al., 2012). Here, for branch, foliage and stem organs we have calculated C_{TLP}, that is C from the initial linear slope describing decline in organ WC with decrease in organ ψ during drying before the leaf ψ_{TLP} (e.g., Bartlett et al., 2012 supplementary information; Bryant et al., 2021) and C_{total}, that is C from the total water lost from first to last measurement (e.g., Gleason et al., 2014). WS (g g^{-1}DM) for branch, foliage and stem organs was then calculated as the total amount of water released over the initial linear region of the curve during drying before the leaf ψ_{TLP} (WS_{TLP}), and as the total amount of water released from first to last measurement (WS_{total}). For physical properties, please see Supporting Information: Table S1.

2.3 | Stem anatomy

For each branch collected for water relations of branches, a paired stem was collected to characterise stem anatomy and allowed to rehydrate overnight as previously described. Before sectioning, three points along the stem (mature, juvenile and young) were selected to capture developmental variation in anatomy, based on stem diameter, proximity to shoot tip, and bark development. Transverse sections (100 µm thick in *A. corniculatum* and 200 µm thick in *R. stylosa*) from each developmental stage were observed under a ZEISS Axiostar Plus epifluorescence microscope (ZEISS). Images were collected using the Halide Mark II Pro Camera app on an iPhone8.

Images were analysed using FIJI image analysis software (Schindelin et al., 2012). Stem area was calculated as the area of a circle for *A. corniculatum* or an ellipse for *R. stylosa* where necessary.

Vessel lumen area was calculated as the area of a circle of each vessel within a 0.25 mm^2 area of xylem tissue from pith to phloem. Tissue layers were defined as per Figure 1 for determination of proportionate contributions to whole-stem area.

2.4 | Hydraulic vulnerability curves

Hydraulic vulnerability was estimated using the pneumatic method which proxies percent air discharge (PAD) for percent loss of hydraulic conductance with declining ψ (PLC; Jansen et al., 2022; Pereira et al., 2016; Sergent et al., 2020; Zhang et al., 2018). Sun-exposed canopy branches >60 cm in length were sampled from trees 2–4 m in height, transported (approximately 30 min) in the dark plastic bags, recut under perfusion solution, and rehydrated. Bench drying and measurement of PAD with declining branch ψ were conducted and analysed using the protocol previously described by Bryant et al. (2021). Briefly, air discharge was measured by exposing a 3.9 mL vacuum reservoir with an absolute pressure of ~40 kPa attached to a pressure transducer (PC140 Series; Omega, CT) to the cut branch end via a three-way stopcock. Pressure was logged every second and initial pressure and pressure after 150 s were recorded. Branches were bench dried and measurements were made at ~1 MPa intervals. For full protocol please see Bryant et al. (2021, Supporting Information).

2.5 | Statistical analyses

Statistical analyses were performed in R (R Core Team, 2023 version 4.3.1). We measured a total of 27 individuals across two species and two salinities from three sites.

2.5.1 | WS, and *C* in branch, foliage and stem organs

A linear mixed model was used to analyse branch level WS and *C* (Figures 2 and 4), with salinity and species as fixed effects, and estuarine site as random intercepts using the lmer() function in the *lmerTest* (Kuznetsova et al., 2017) and *lme4* package (Bates et al., 2015). To then assess the contribution made by foliage and stem organs to branch WS and *C* (Figures 2 and 4), a linear mixed model was used with salinity, species and organ (foliage and stem) as fixed effects, and estuarine site and individual as random intercepts. The anova() function was used to assess the significance of main effects and interactions at the $p < 0.05$ level.

2.5.2 | Sources of stem *C*

A linear model was used to test the effects of anatomical traits on stem *C*, with species as a fixed effect (Figure 5). Slopes and differences between slopes (species by anatomical trait interaction) were considered significant at the $p < 0.05$ level.

2.5.3 | Hydraulic vulnerability curves

PAD was plotted against ψ values and fitted with a reparameterised Weibull model (Ogle et al., 2009) with 95% bootstrap confidence intervals generated with 1000 resamples using the *fitplc* package (Duursma & Choat, 2017). Model fit was assessed by plotting observed conductance against model predicted curves and significance was assessed using the *smart* package (Warton et al., 2012). Parameters including P12 and P50 (Figure 6) were determined using the *fitplc* package.

Model fit was assessed through a number of diagnostic tests including diagnostic residual plots and the Shapiro–Wilk test, and where necessary dependent variables were log transformed to improve model fit. The *emmeans* R package (Lenth, 2020) was used for pairwise comparisons and to produce model estimated marginal means, trendlines and standard error (SE) for figures. Figures were produced using the package *ggplot2* (Wickham, 2016).

3 | RESULTS

3.1 | Foliage and stem contribution to total branch capacitance (C_{total})

The proportional contributions that stem and foliage make to the WC of the whole branch during drying can be shown by plotting stem and foliage WC relative to the initial measurement where whole branch relative water content (RWC) was 100% (Figure 2b). When branch RWC was 100% the foliage contributed between 55% (±7) of branch RWC in *A. corniculatum* at low salinity and 69% (±9) of branch RWC in *R. stylosa* at high salinity, reflecting the greater proportion of branch saturated WC held in the foliage than the stem. C_{total} and the relative contributions of foliage and stem to branch C_{total} were calculated from saturation to final measurement (Figure 2c). There was a significant species by salinity effect ($p = 0.007$) whereby branch C_{total} declined across low and high salinity in *A. corniculatum* but increased across low and high salinity in *R. stylosa* (Figure 2c). The foliage contributed 50% (±4) of the branch C_{total} at low salinity on average across both species, compared with 66% (±5) at high salinity. While foliage and stem contribution to branch C_{total} did not significantly differ at low salinity, there was a significant organ by salinity effect ($p = 0.013$) due to the greater overall contribution of foliage than stem at high salinity ($p = 0.013$).

3.2 | Water relations of branch, foliage and stem organs

Individual drying of the two main organs of the branch can be assessed by plotting the WC of each organ relative to their own initial measurement at 100% RWC (Figure 3). Water release curves for branch and foliage had two phases of RWC decline similar to a two-domain leaf PV curve. In the first phase there was a greater decrease

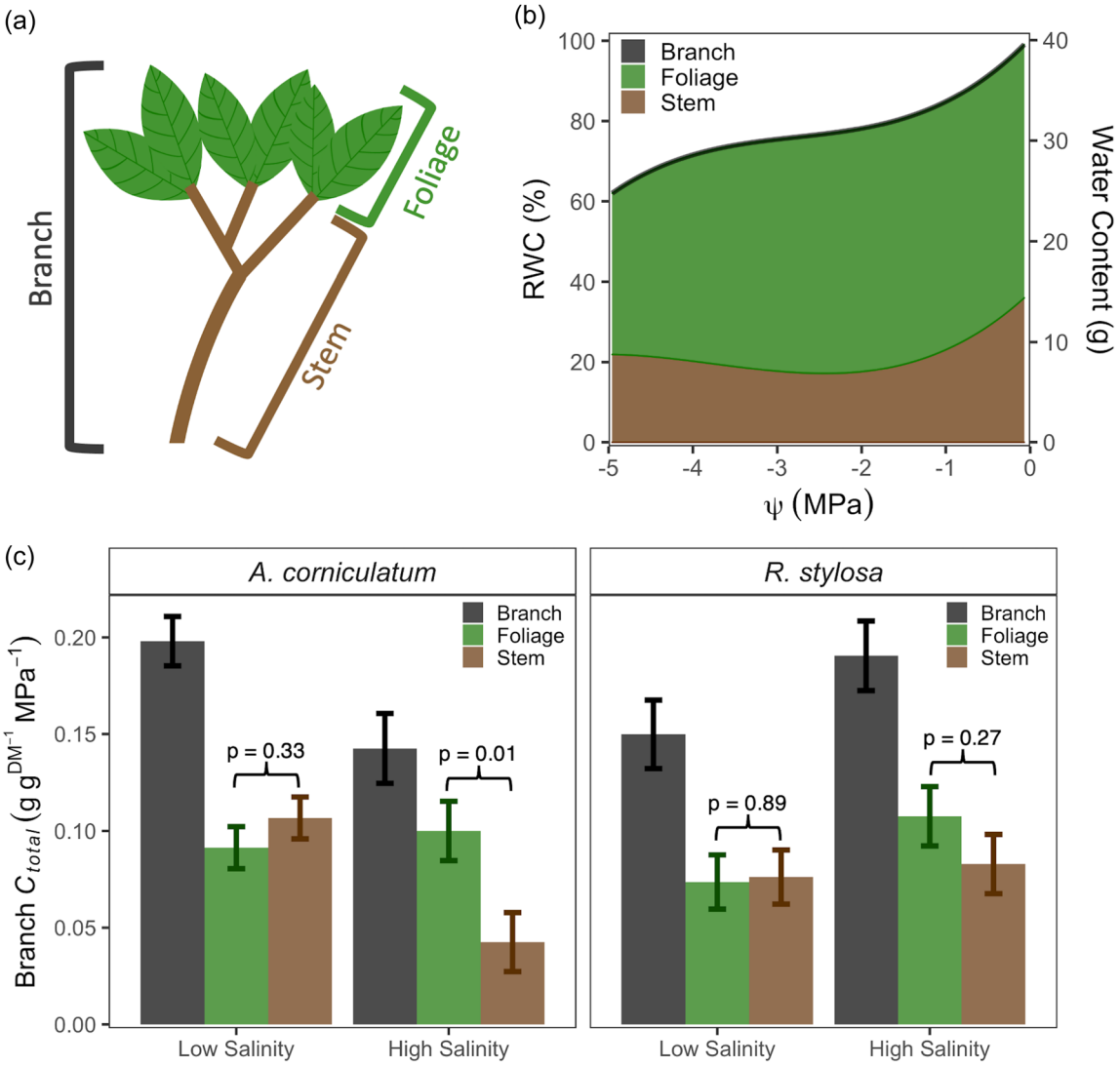

FIGURE 2 Change in branch RWC (black) and its distribution between foliage (green) and stem (brown) organs during drying in *Aegiceras corniculatum* and *Rhizophora stylosa*. (a) Diagram defining the contribution of foliage and stem organs to a branch. (b) Exemplary branch water release curve showing the relative contribution of foliage and stem organs to decline in whole branch RWC with decreasing water potential (ψ) during drying. Note the *y*-axis showing RWC (right) is mirrored by the corresponding water content (left). (c) Proportional contribution of foliage and stem organs to total branch capacitance (Branch C_{total}) calculated as gram per gram branch dry mass per MPa from saturation to final measurement in *A. corniculatum* collected from low ($n = 10$) and high salinity ($n = 5$), and in *R. stylosa* collected from low ($n = 7$) and high salinity ($n = 10$) sites along the Daintree River. Values for branch C_{total} are estimated marginal means ± SE from a linear mixed model with salinity and species as fixed effects, and estuarine site as random intercepts. Values for foliage and stem contribution to branch C_{total} are estimated marginal means ± SE from a linear mixed model with salinity, species and organ as fixed effects, and estuarine site and individual as random intercepts. Corresponding observed means ± SE are given in Supporting Information: Table S3 and results from associated ANOVAs in Supporting Information: Table S2. RWC, relative water content. [Color figure can be viewed at wileyonlinelibrary.com]

in ψ for a small change in foliage and branch RWC, which in leaf PV curves is driven mainly by decline in turgor during water loss from living cells. In the second domain ψ and RWC declined together, characterised by decreasing osmotic potential in leaf PV curves. In leaves, the intersection between these two domains represents the turgor loss point (leaf ψ_{TLP}), which when plotted onto branch and foliage water release curves (blue line, Figure 3) coincides closely with the inflection point between the two phases of water loss for foliage and often coincides for branch.

However, stem water release curves followed a different pattern of water release, which occurred over three phases and varied between high and low salinity (Figure 3). At low salinity, *C* was smaller in the first linear phase than in the subsequent linear phase. At high salinity, *C* of the initial linear phase was greater than the subsequent linear phase. Surprisingly, in the third phase of the stem water release curve, stem RWC increased as ψ continued to decline with dehydration. This increase in stem RWC was more prevalent at high than low salinity, observed in 50% and 57% of low salinity individuals

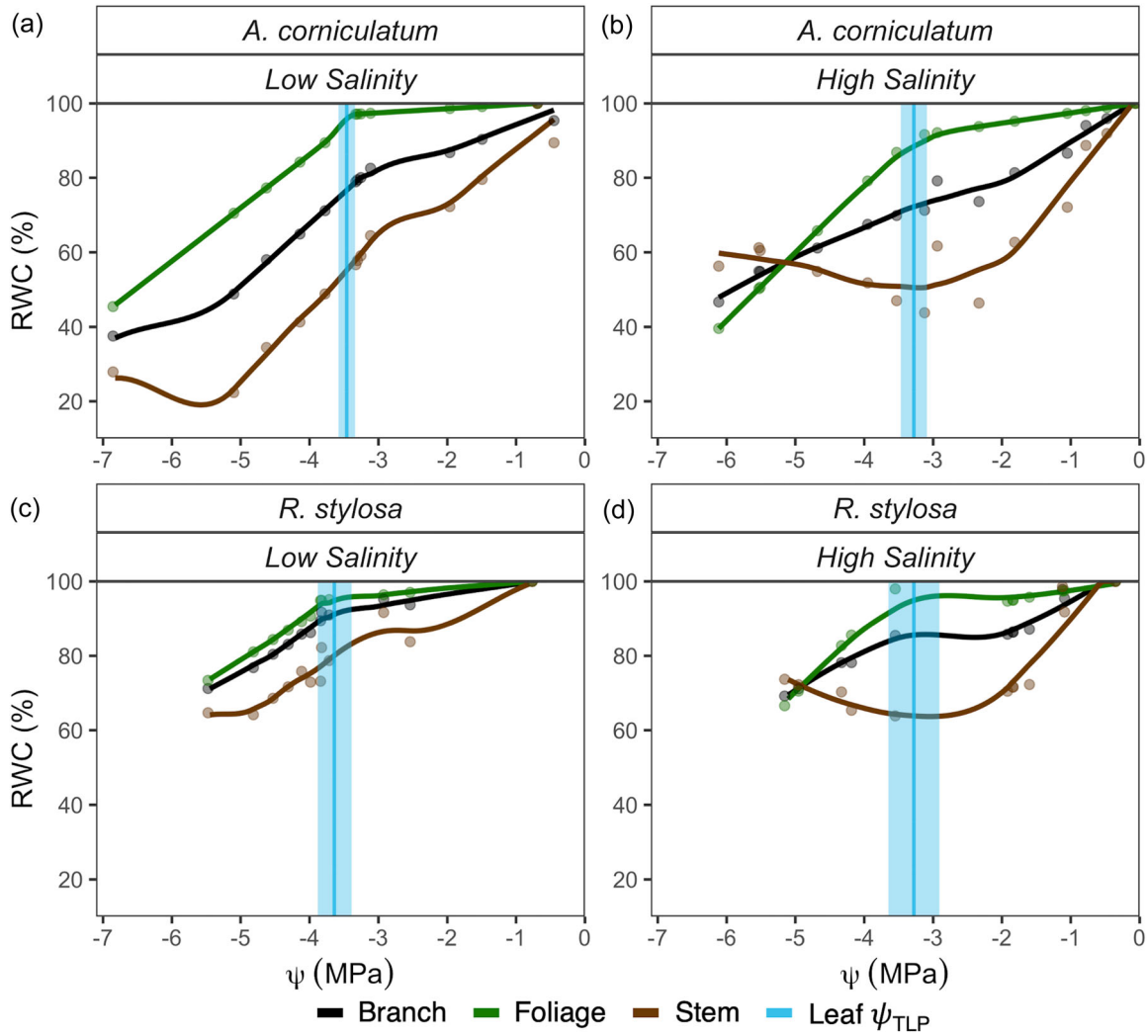

FIGURE 3 Representative water release curves of branch (black), foliage (green), and stem (brown) organs of *Aegiceras corniculatum* (a, b) and *Rhizophora stylosa* (c, d) showing change in relative water content (RWC) as water potential (ψ) decreases during drying at low (a, c) and (b, d) high salinity. Branch and its composite foliage and stem are presented relative to their own initial measurement at 100% RWC. Points depict data from measurements of *A. corniculatum* and *R. stylosa* branch, foliage, and stem RWC at a given ψ made on a single individual of each species from low and high salinity. A loess running average curve was then fitted for each organ. Blue band and shading indicates the mean leaf $\psi_{TLP} \pm$ SE from paired pressure-volume measurements from an individual leaf taken from each branch. Water release curves of branch, foliage, and stem organs for each individual of *A. corniculatum* and *R. stylosa* can be viewed in Supporting Information: Figure S1. [Color figure can be viewed at wileyonlinelibrary.com]

of *A. corniculatum* and *R. stylosa* respectively, but 100% of stems of both species at high salinity. Indeed, the increase in stem RWC at high salinity was coincident with leaf ψ_{TLP} and corresponded with a greater decrease in foliage RWC for a given change in foliage ψ, suggesting reallocation of water from the foliage to the stem in that instance.

Where applicable, reallocation of foliage water to stems was calculated as the difference between the lowest value of stem RWC and the highest subsequent value of stem RWC. Reallocation of water to the stem was greatest in *A. corniculatum* at high salinity, increasing stem RWC by 21.1% (±2) compared with 12.7% (±5) in *R. stylosa*. At low salinity reallocation increased stem RWC by 12.0% (±8) in *A. corniculatum* and 1.6% (±2) in *R. stylosa*.

3.3 | *C* and WS in branch, foliage and stem organs

C_{TLP} and WS_{TLP} were calculated from the initial linear phase of water release before leaf ψ_{TLP} in two ways. First, C_{TLP} and WS_{TLP} were calculated as branch RWC release before leaf ψ_{TLP} (Figure 4a,c) giving the proportionate contributions of foliage and stem to branch C_{TLP} and WS_{TLP}. Second, C_{TLP} and WS_{TLP} were calculated as water released from each organ per gram organ DM before leaf ψ_{TLP} (Figure 4b,d) giving values for each organ relative to itself, rather than relativised against branch, and referred to here as 'absolute' C_{TLP} and WS_{TLP}. Branch C_{TLP} (% RWC_{Branch}) did not significantly differ with salinity in either species. However, the relationship between branch C_{TLP} and salinity differed between species ($p = 0.0002$) tending to decrease with salinity in *A. corniculatum* but increase with salinity in

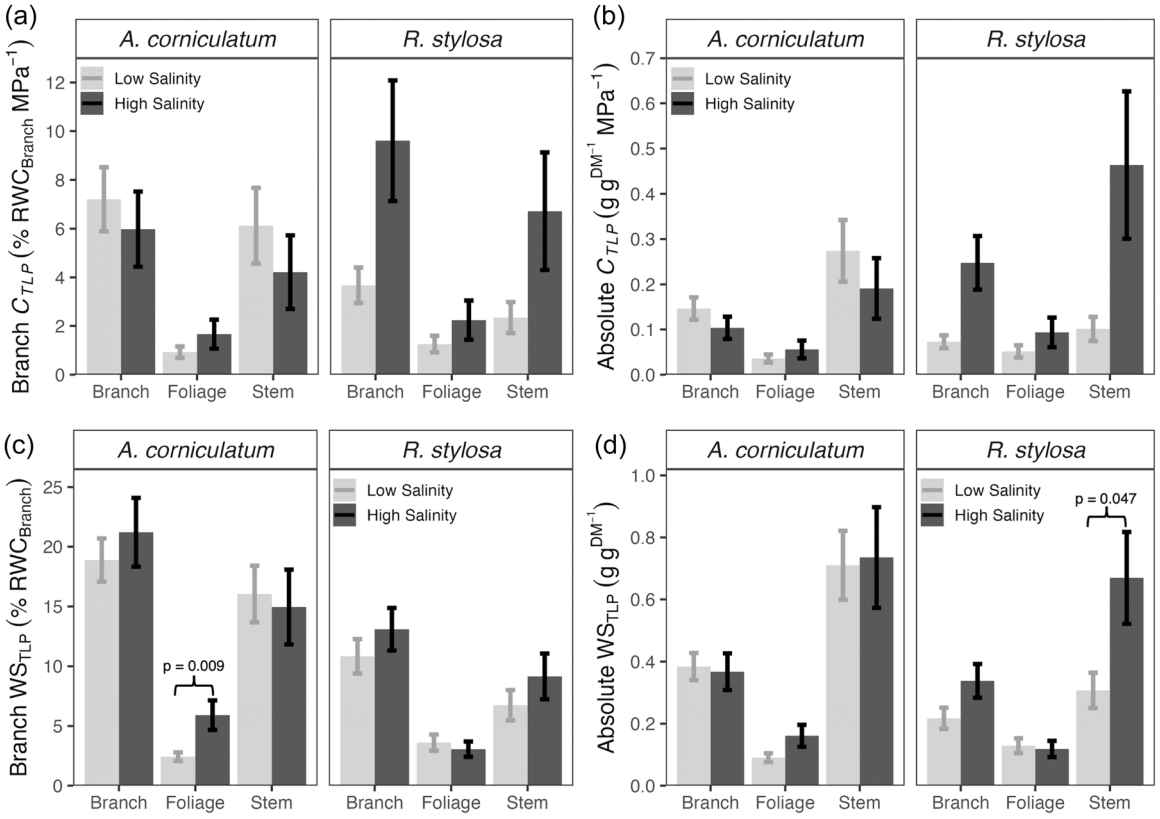

FIGURE 4 Shifting contribution of foliage and stem organs to branch capacitance (C_{TLP}) and water storage (WS_{TLP}) calculated from the initial linear phase of water release from saturation to the leaf water potential at the turgor loss point in *Aegiceras corniculatum* and *Rhizophora stylosa* grown at low (grey) and high (black) salinity. Figure shows proportionate contribution of foliage and stem organs to (a) branch C_{TLP} and (c) branch WS_{TLP} calculated as a percent of branch relative water content (% RWC_{Branch}), and absolute branch, foliage and stem (b) C_{TLP} and (d) WS_{TLP} calculated as gram per gram organ DM (g gDM^{-1}) where each organ was calculated relative to itself rather than to branch. Values for branch are estimated marginal means ± SE from a linear mixed model with salinity and species as fixed effects, and estuarine site as random intercepts. Values for foliage and stem are estimated marginal means ± SE from a linear mixed model with salinity, species and organ as fixed effects, and estuarine site and individual as random intercepts. Data were log transformed for analyses to account for nonnormality of model residuals. Values are for *A. corniculatum* collected from low (n = 10) and high salinity (n = 5), and *R. stylosa* collected from low (n = 7) and high salinity (n = 10) sites along the Daintree River. Corresponding observed means ± SE are given in Supporting Information: Table S3 and results from associated ANOVAs in Supporting Information: Table S4. [Color figure can be viewed at wileyonlinelibrary.com]

R. stylosa. As a result, branch C_{TLP} was greater in *A. corniculatum* than *R. stylosa* at low salinity (p = 0.0005) while the inverse was true for high salinity (p = 0.029, Figure 4a). There was no significant effect of salinity or species on branch absolute C_{TLP}; however, the effect of salinity differed by species such that branch absolute C_{TLP} at low salinity was greater in *A. corniculatum* than *R. stylosa* (p = 0.002, Figure 4b), while the opposite was true at high salinity (p = 0.002).

Branch WS_{TLP} (% RWC_{Branch}) did not differ significantly by salinity in either species, but did differ by species (p = 0.0003) such that branch WS_{TLP} was greater in *A. corniculatum* than *R. stylosa* at both low (p = 0.002) and high salinity (p = 0.02, Figure 4c). Likewise, there was no overall effect of salinity on branch absolute WS_{TLP} (Figure 4d). Overall, branch absolute WS_{TLP} was greater in *A. corniculatum* than *R. stylosa* (p = 0.03).

Although the proportional contribution of foliage to branch C_{total} was equal to or greater than the stem (Figure 2), the contribution made by foliage and stem to branch WC released during drying shifted as drying progressed. In both species, the stem contributed a greater proportion to branch C_{TLP} and WS_{TLP} than the foliage (p < 0.0001, Figure 4a,c), contributing 76% (±4) of branch WS_{TLP} released at low salinity and 71% (±4) at high salinity (Supporting Information: Tables S1 and S2). However, following leaf ψ_{TLP}, foliage water release was greater than the contribution made by the stem accounting for 62% (±5) at low salinity and 98% (±7) at high salinity of the further decline in branch RWC. Consequently, 72% (±6) of stem WS_{total} was released before the leaf ψ_{TLP}, while 84% (±3) of foliage WS_{total} was released following leaf ψ_{TLP}.

3.4 | Sources of stem C_{TLP}

Stem C_{TLP} in *R. stylosa* increased significantly with the proportion of inner bark and cortex in the stem and decreased significantly with xylem tissue contribution to the stem, while in *A. corniculatum*, stem

C_{TLP} decreased with the proportion of inner bark and cortex in the stem but was not significant (Figure 5a,b). A slight positive relationship with xylem was the strongest positive relationship found between *A. corniculatum* and any stem anatomical traits. As a result, the species differed significantly in their relationships between stem C_{TLP} and inner bark and cortex and xylem (Figure 5ab).

The xylem contribution to stem C_{TLP} was further examined through the proportion of vessel, fibre and parenchyma tissue comprising the xylem area. Despite the overall negative relationship with total xylem tissue, *R. stylosa* stem C_{TLP} was positively related to vessel contribution to xylem area and parenchyma as a proportion of xylem area (Figure 5c,e), such that when contribution of parenchyma

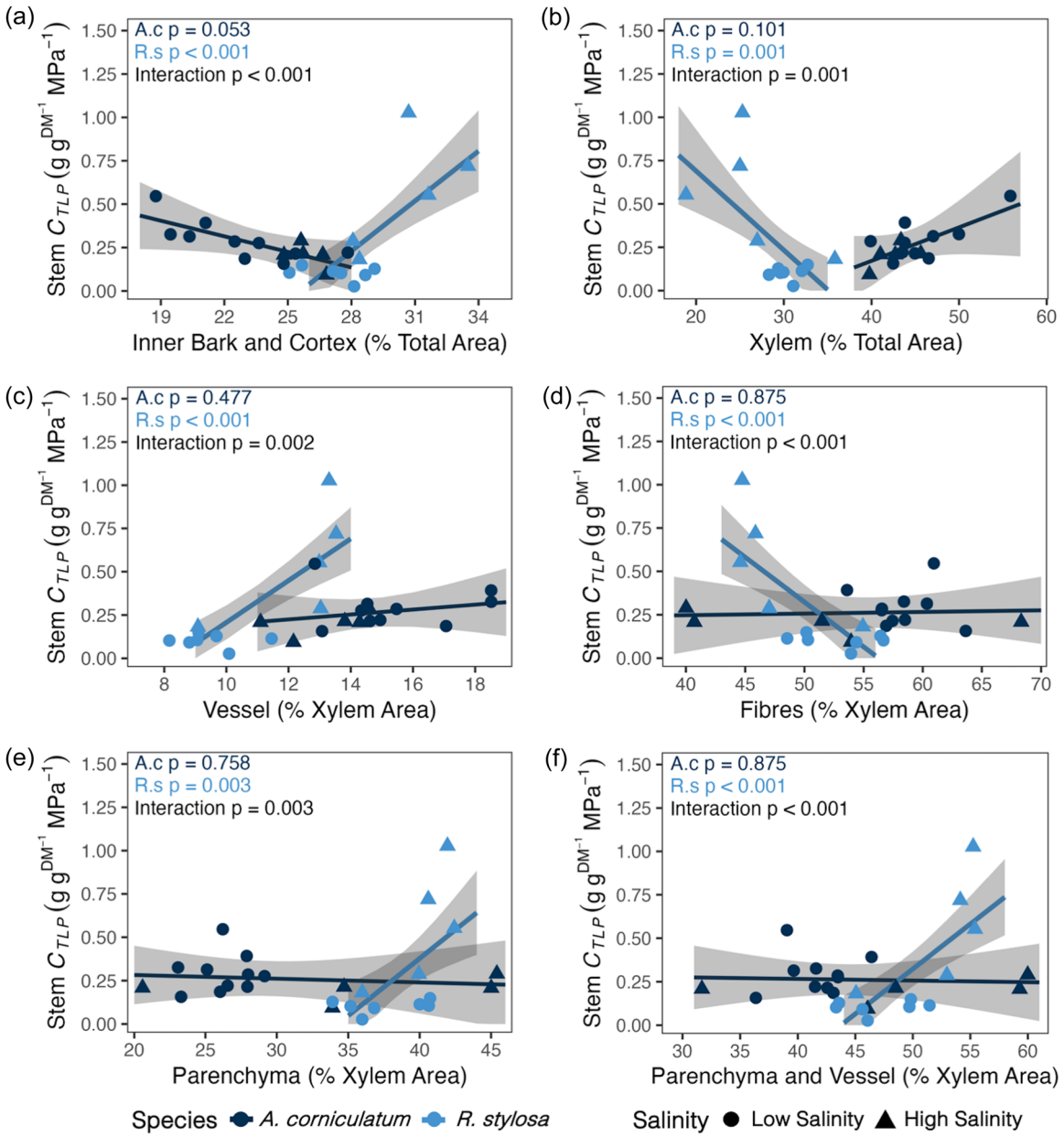

FIGURE 5 Key stem anatomical traits as sources for stem capacitance calculated from the initial linear phase of stem water release before leaf water potential at the turgor loss point (C_{TLP}, g gDM^{-1} MPa^{-1}) in *Aegiceras corniculatum* and *Rhizophora stylosa*. Relationship between stem C_{TLP} and (a) combined inner bark and cortex tissue percent of total stem area, (b) xylem tissue percent of total stem area, (c) vessel percent of xylem area, (d) fibre percent of xylem area, (e) parenchyma percent of xylem area, and (f) combined parenchyma and vessel percent of xylem area. Species, anatomical trait and species by anatomical trait trendlines are estimated marginal means from a linear model with species as fixed effects. Shading indicates 95% confidence intervals, with associated *p* values indicating within-species significance included above. Datapoints represent individual measurements of *A. corniculatum* collected from low (n = 10, dark blue) and high salinity (n = 5, light blue), and of *R. stylosa* collected from low (n = 7, dark blue) and high salinity (n = 10, light blue) sites along the Daintree River. For underlying stem anatomical characteristics please see Supporting Information: Tables S5 and S7. Results from associated estimated marginal trendlines are given in Supporting Information: Table S6. [Color figure can be viewed at wileyonlinelibrary.com]

and vessels were combined, *R. stylosa* stem C_{TLP} had a significant positive relationship (Figure 5f). However, stem C_{TLP} in *R. stylosa* was negatively related to fibre contribution to xylem area (Figure 5d) possibly driving the overall negative association with xylem area. As no strong relationship was found between *A. corniculatum* and any stem anatomical traits, *A. corniculatum* and *R. stylosa* had significantly different relationships with vessel, and parenchyma area which drove a significant difference between species in vessels and parenchyma area combined. Similarly, fibre contribution to xylem area varied significantly between species.

3.5 | Hydraulic vulnerability curves

P12 and P50 were approximately 1.7 MPa lower at high than low salinity across both *A. corniculatum* and *R. stylosa* (Figure 6), reducing vulnerability to stem embolism at high salinity. However, the slope at P50 was slightly greater at high than low salinity in *A. corniculatum*, despite lower P12 and P50. The opposite was true for stems of *R. stylosa* where the slope at P50 at low salinity indicated greater potential for rapid development of xylem embolism as dehydration progressed beyond P12 compared with stems from high salinity, and therefore reduced risk of runaway embolism at high salinity. P12 and P50 were lower in *A. corniculatum* than *R. stylosa* at both low and high salinity, indicating greater resistance to embolism development in *A. corniculatum* stems.

The HSM in *R. stylosa* was slightly smaller at low salinity (2.23 MPa) than at high salinity (2.47 MPa), as was the case for the HSM in *A. corniculatum* (4.17 and 4.25 MPa at low and high salinity, respectively, Figure 6). Conversely, the TSM was largest at low salinity with an average of 3.5 MPa (±0.1) across both species, and smallest at high salinity with an average of 1.6 MPa (±0.2) across both species (Figure 6).

4 | DISCUSSION

The present study uses a holistic approach to investigate plasticity in branch, foliage and stem water relations, shifting organ-level contributions to branch water release during drying, and TSM and HSM among two mangrove species growing at high and low salinities. C_{TLP} and WS_{TLP} were greater in the stem than the foliage in both species, buffering stem xylem against embolism formation. Yet, in both species dynamic changes in *C* during drying conserved WC in the stem at the expense of the foliage as branch water loss progressed during drying, and provides evidence for hydraulic redistribution of water from the foliage to the stem. Plasticity in P12 and P50 decreased hydraulic vulnerability in trees growing at high salinity; however, the TSM declined as salinity increased, increasing the vulnerability of living tissue to water stress. Combined our results highlight the complex interplay between plasticity in organ-level water relations and plasticity in hydraulic vulnerability in the maintenance of stem hydraulic function in mangroves distributed across salinity gradients.

4.1 | Shifting sources of water release during dehydration contribute to the maintenance of hydraulic function while conserving RWC in the stem

Responses of branch C_{TLP} and WS_{TLP} to salinity differed between *R. stylosa* and *A. corniculatum*, but would contribute to the maintenance of hydraulic function when water availability was limited by high salinity in both species (Figure 4). In *R. stylosa*, increased branch C_{TLP} between low and high salinity would increase the capacity to buffer against xylem ψ gradients that can cause embolism (Meinzer et al., 2003, 2008; Preisler et al., 2022), providing greater hydraulic safety where water availability was most limited. Conversely, branch C_{TLP} in *A. corniculatum* decreased between low and high salinity, decreasing buffering capacity. However, while branch C_{TLP} was greater in *R. stylosa* than *A. corniculatum* at high salinity, both species had similar branch WS_{TLP} available for capacitive release at high salinity (Figure 4). A similar volume of water released more slowly would allow for smaller but more prolonged buffering effects as dehydration progressed in *A. corniculatum*, compared with rapid discharge of stored water in *R. stylosa*. This interplay between WS_{TLP} and C_{TLP} may explain the occurrence of P12 and P50 at more negative ψ in *A. corniculatum* than *R. stylosa* (Figure 6).

Although at high salinity foliage contributed a greater proportion of branch C_{total} than the stem, contrary to our hypothesis stem C_{TLP} and WS_{TLP} were greater than the foliage at both salinities (Figure 4), accounting for 83% of branch WS_{TLP} released and 81% of stem WS_{total}. In other words, the stem released a greater proportion of its own WC more rapidly than the foliage over the initial phase of water release before leaf ψ_{TLP}. However, following exhaustion of WS_{TLP} the stem contributed just 38% of further branch WC released at low salinity and 0% at high salinity on average across both species, shifting to foliage as the capacitor as dehydration became more severe (Figure 7).

Similar to the increased foliage contribution to branch C_{total} at high salinity measured here, Bryant et al. (2021) found that increased leaf *C* in the late dry season buffered against declining ψ such that vulnerability to hydraulic failure reduced. Zimmermann (1983) first proposed that 'plant segmentation' allows a plant to conserve organs critical to long term plant survival (roots and stems) by sacrificing organs of lesser investment that are more easily replaced (leaves). The results presented here are consistent with this theory, whereby large stem C_{TLP} would enable rapid mobilisation of water from storage tissues. At the same time, preferentially losing water from the foliage following leaf ψ_{TLP} would reduce the risk of damage to the stem as branch drying progressed. Combined, stem C_{TLP} would sustain rates of water use for carbon gain, while foliage water release would prevent xylem embolism and maintain water content in the stem where the consequences to the plant would be greatest (Brodersen et al., 2010; Nardini et al., 2011; Robert et al., 2009; Salleo et al., 2009; Sevanto et al., 2014).

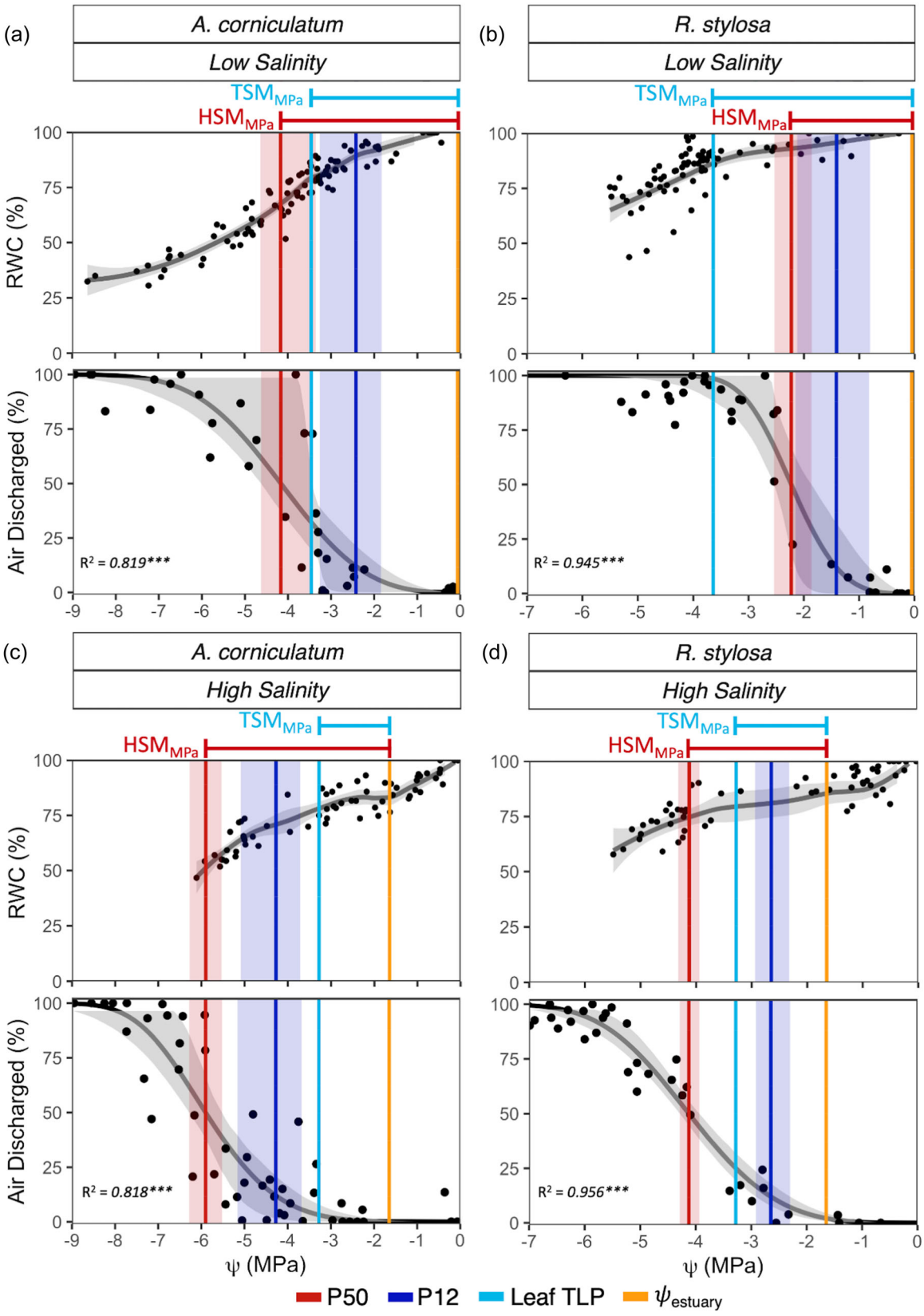

FIGURE 6 (See caption on next page).

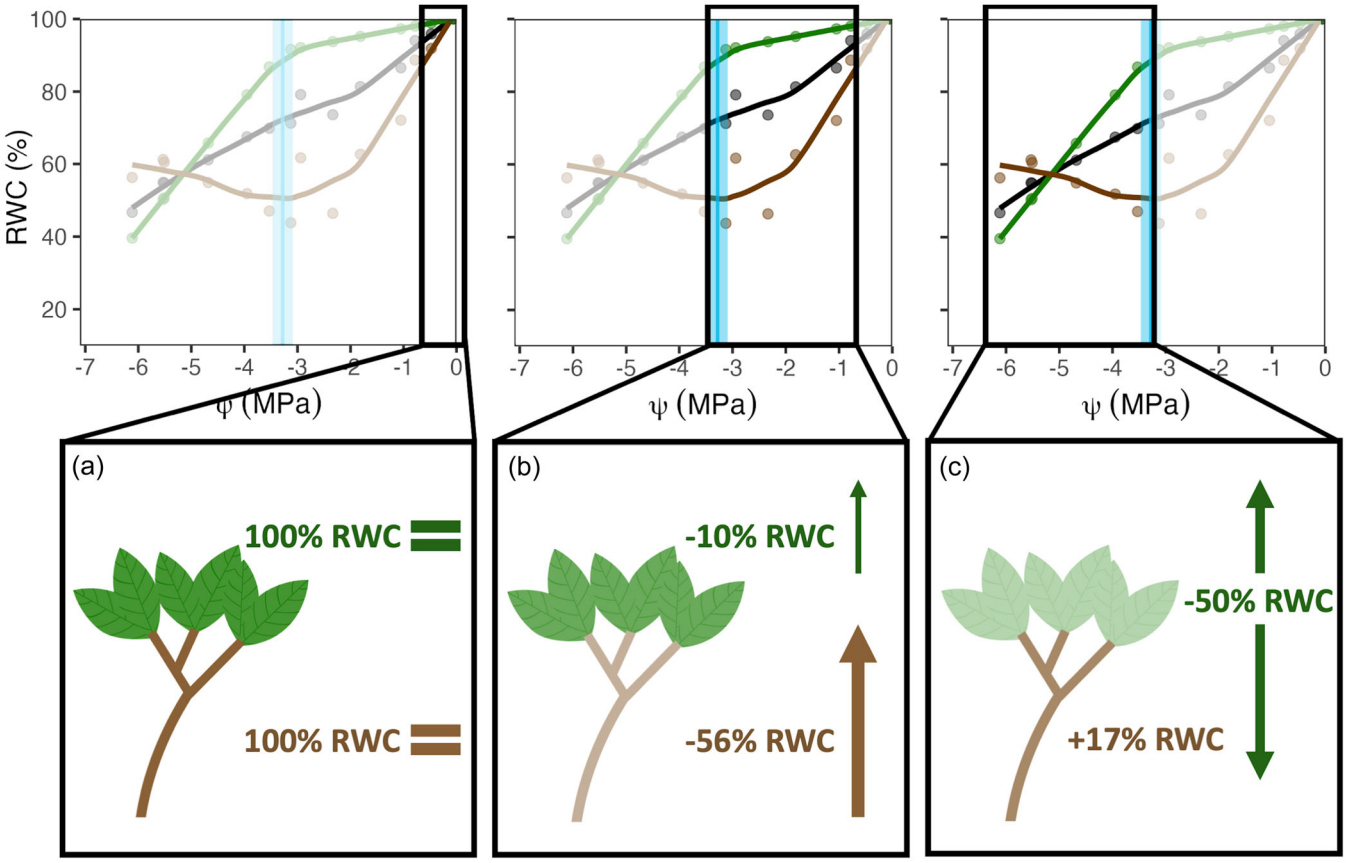

FIGURE 7 Illustrative diagram showing hydraulic redistribution of water from the foliage to the stem as branch water loss progressed beyond the water potential at the leaf turgor loss point (ψ_{TLP}). Top panels show a representative water release curve of branch (black), foliage (green), and stem (brown) organs of *Aegiceras corniculatum* at high salinity, with blue band and shading indicating the mean leaf ψ_{TLP} ± SE from Figure 3. Lower panels show (a) before dehydration foliage and stem are at 100% relative water content (RWC), (b) as dehydration progresses before the leaf ψ_{TLP} the stem contributes the majority of water lost from the branch reducing the RWC in the stem by 56%, with a smaller 10% contribution to branch water loss made by the foliage, (c) upon reaching the leaf ψ_{TLP} decline in stem RWC ceases and instead increases by 17%, coinciding with an increase in water lost from the foliage whereby foliage RWC declined by 50% driving the continued decline in branch RWC. Upward arrows indicate water loss to the atmosphere while downward arrows indicate redistribution of water from foliage to stem. Black boxes around upper panels represent the corresponding range of ψ on the water release curve over which the change in RWC in foliage and stem organs occurred. Values for change in RWC in foliage and stem organs are derived from the individual pressure-volume curve shown. [Color figure can be viewed at wileyonlinelibrary.com]

4.2 | Stem C_{TLP} increased with the proportion of living stem tissue in *R. stylosa* but not *A. corniculatum*

Given the large proportion of whole branch C_{TLP} contributed by the stem, the relationship between stem C_{TLP} and anatomy was investigated to identify possible source tissues (Figure 5). Stem C_{TLP} in *R. stylosa* was positively related to the proportion of living tissue in the stem as hypothesised, supporting elastic living tissue as the dominant source of WS in the stem (Goldstein et al., 1998; Pfautsch et al., 2015; Treydte et al., 2021). In contrast, no positive correlations

FIGURE 6 Stem percent air discharged (PAD) and branch water released with decreasing water potential (ψ) during drying in *Aegiceras corniculatum* (a, c) and *Rhizophora stylosa* (b, d) collected from low (a, b) and high (c, d) salinity on the Daintree River. Upper panels show decreasing average branch relative water content (RWC) during drying. Points depict water relations data from individuals of *A. corniculatum* (n = 10 from low salinity and n = 5 from high salinity), and of *R. stylosa* (n = 7 from low salinity and n = 5 from high salinity), a loess running average curve was then fitted for each species and salinity. Lower panels show increasing stem PAD during drying; points depict hydraulic vulnerability data from individuals of *A. corniculatum* (n = 6 from low salinity and n = 5 from high salinity), and of *R. stylosa* (n = 6 from low salinity and n = 4 from high salinity). Grey shading shows the 95% CI. Dark blue vertical line and shading gives the mean ψ ± 95% CI at which 12% loss of stem hydraulic conductance occurs (P12, Supporting Information: Table S8). Red vertical line and shading gives the mean ψ ± 95% CI at which 50% loss of stem-hydraulic conductance occurs (P50, Supporting Information: Table S8). Light blue vertical line gives the mean ψ at leaf turgor loss (ψ_{TLP}) from paired leaf pressure-volume curves. Mean leaf ψ_{TLP} ± SE previously shown in Figure 3. Yellow vertical line gives mean ψ of the estuarine water ($\psi_{estuary}$). Light blue horizontal bar at the top of each panel shows the turgor safety margin (TSM, the range of ψ between $\psi_{estuary}$ and ψ_{TLP}). Red horizontal bar at the top of each panel shows the hydraulic safety margin (HSM, the range of ψ between $\psi_{estuary}$ and the ψ at P50). [Color figure can be viewed at wileyonlinelibrary.com]

were found between stem C_{TLP} and anatomy in *A. corniculatum*, raising the possibility that water discharged from storage may be sourced broadly from both living tissues and apoplastic spaces. Indeed, studies have suggested that water released from the apoplast in xylem tissues through cavitation of fibres and vessels may also act as a capacitor (Baer et al., 2021; Cai et al., 2014; Gessler, 2021; Knipfer et al., 2019; Yazaki et al., 2020; Zweifel et al., 2014), with spatial variation in cavitation enhancing the maintenance of hydration required for survival of critical living tissues during extreme drought conditions (Barigah et al., 2013). Further research is required to understand the patterns of water loss and retention within stems of intact plants in relation to their function under increasing water stress induced by drought and salinity.

4.3 | Following leaf TLP, reallocation of water from the foliage increased RWC in the stem

Our results suggest that dynamic reallocation of water during dehydration may be a central process in maintaining stem hydraulic function. We measured an increase in stem RWC following leaf ψ_{TLP}, consistent in both species with particular prevalence at high salinity (Figure 3). This increase in RWC tended to coincide with a greater decrease in foliage RWC for a given change in ψ suggesting reallocation of water from the foliage to the stem (Figure 7).

Epila et al. (2017) found evidence for internal spatial reallocation of leaf water within branches that would delay desiccation and prolong carbon uptake under drought conditions. They observed that as bench-top dehydration progressed in branches of *Maesopsis eminii*, ψ in some leaves reduced as expected, while ψ increased in others. The authors hypothesised that as dehydration progressed, some leaves were isolated from water supply and this water was redirected to those still hydraulically connected. We propose a similar process whereby water may have been redistributed to the stem during dehydration through release of water from progressive cavitation of leaf vessels, and movement of leaf water through symplastic networks such as phloem. Indeed, the range of ψ over which water was reallocated from foliage to stems at high salinity (Figure 3) overlapped with those at which PAD increased from 12% to 50% (Figure 6). Further research is required to determine the extent to which reallocation of water occurred through apoplastic or symplastic pathways. Reallocation of foliage water to the stem that increased stem RWC by approximately 21.5% in *A. corniculatum* and 9.5% in *R. stylosa*, would contribute to the survival of stem tissues. Therefore, metrics commonly used to assess drought vulnerability such as hydraulic vulnerability may not capture true vulnerability to drought without also taking into account water management strategies (Epila et al., 2017).

Although reallocation occurred in all individuals measured at high salinity, a greater increase in stem RWC was measured in *A. corniculatum*. *A. corniculatum* has a lower tolerance of high salinity than *R. stylosa* (Ball, 1988b), likely resulting in a greater emphasis in *A. corniculatum* on stem tissue survival and prevention of runaway embolism over growth of the foliage at high salinity. In this way, reallocation of water from the foliage to the stem can be viewed as an extension of the plant segmentation theory (Zimmermann, 1983), that could contribute to the conservation of the stem during daily function and extreme events. Given the consistency with which this phenomenon was observed in both species at both salinities, and the observation that increased stem RWC only occurred after the leaf ψ_{TLP}, reallocation of water warrants further investigation.

4.4 | Plasticity in P12 and P50 reduced hydraulic vulnerability at high salinity

As hypothesised, both *A. corniculatum* and *R. stylosa* adjusted P12 and P50 by approximately −1.7 MPa between low and high salinity sites (Figure 6). The evidence for plasticity in stem P50 within species to suit different environmental conditions is highly variable, ranging from little evidence of plasticity (Bittencourt et al., 2020; Choat et al., 2012; Ladjal et al., 2005; Lamy et al., 2014; Martínez-Vilalta et al., 2009; Mencuccini & Comstock, 1997) to significant shifts in hydraulic vulnerability in response to environmental change, depending on the species studied (Beikircher & Mayr, 2009; Feng et al., 2023; Jacobsen et al., 2014; Jacobsen et al., 2007; Kolb & Sperry, 1999; Ladjal et al., 2005; Schuldt et al., 2016; Stiller, 2009). We provide evidence in two mangrove species that P12 and P50 are highly adjustable, which would confer greater hydraulic safety where salinity limits water availability, consistent with the wide distributions of these species across salinity gradients. It remains unknown to what extent P12 and P50 are plastic within an individual in response to increasing salinity during drought.

Xylem vessels were slightly smaller at high salinity in *A. corniculatum*, potentially facilitating plasticity in P12 and P50, but not in *R. stylosa*. Evidence suggests that some species can modify vulnerability to embolism by altering the chemical and structural composition of the pit membranes, changing their porosity and reducing the likelihood of air seeding (Choat et al., 2008; Herbette et al., 2015; Jansen et al., 2009; Pereira et al., 2018b, 2018a; Schenk et al., 2017). Therefore, changes in the pit membranes that connect conduits both radially and axially may have facilitated the reduced hydraulic vulnerability at high salinity.

4.5 | Greater plasticity in HSMs than TSMs reduced hydraulic vulnerability as salinity increased

Contrary to our hypothesis, greater plasticity in P50 than leaf ψ_{TLP} maintained HSM as salinity increased (Figure 6). Although HSM were slightly smaller at low than high salinity, the risk of severe water stress is low due to the upstream position of the site away from inundating seawater. At high salinity, large HSMs reduced hydraulic vulnerability such that plausible increases in salinity to seawater (osmotic potential of −2.4 MPa) would alone be unlikely to cause

sufficient water deficit for hydraulic failure. However, smaller TSM at high salinity increased turgor vulnerability to water stress. Therefore, under extreme dry-season conditions it is possible that turgor vulnerability poses a greater risk to function than hydraulic vulnerability, as the likelihood of cellular damage such as electrolyte leakage increases following turgor loss and can lead to complete membrane failure and plant death with further dehydration (Guadagno et al., 2017).

Indeed, studies have found that measures of vulnerability in living tissue better predict mortality during drought than hydraulic vulnerability. For example, drought-induced mortality increased as the RWC declined below the TLP in *Pinus ponderosa* (Sapes & Sala, 2021), possibly due to extensive cell damage, as measured in Lavender following the exhaustion of stored water that prevented recovery during drought (Lamacque et al., 2020). Furthermore, Guadagno et al. (2017) found that membrane failure most precisely predicted plant mortality, with failure of meristematic tissue being the final response to drought stress, and Preisler et al. (2021) found that the cessation of radial flow preceded mortality and was irreversible in the stem, such that maintenance of radial flow was critical for drought recovery. Therefore, a greater focus on the vulnerability of living tissue is required to understand recovery and mortality during water stress. It is likely that the relationships between hydraulic and turgor vulnerability become increasingly evident over greater extremes in salinity than were measured here.

5 | CONCLUSION

Branch water release conserved WC in the stem at the expense of the foliage during drying. This outcome is directly consistent with notions of plant segmentation and provides evidence of hydraulic redistribution from the foliage to the stem during drying. In addition, we found substantial plasticity within species in P12 and P50 in response to salinity. This plasticity in hydraulic vulnerability combined with dynamics of stem *C* and WS enabled increases in hydraulic safety at high salinity, suggesting that measurements of hydraulic vulnerability alone may underestimate tolerance to drought. However, reduced TSMs at high salinity would increase the vulnerability of symplastic tissue to cellular damage. Therefore, turgor vulnerability may determine drought tolerance in mangroves. Our results highlight the complex interplay of plasticity in organ-level water relations with hydraulic vulnerability in the maintenance of stem hydraulic and turgor-dependent function in mangroves distributed along salinity gradients.

ACKNOWLEDGEMENTS

The authors acknowledge the Kuku Yalanji and the Ngunnawal and Ngambri peoples, the traditional custodians of the land on which this work was conducted. We pay our respects to them and their cultures and to elders both past and present. The authors thank the Australian Research Council for support through Discovery Project Grant DP180102969 awarded to Marilyn C. Ball and Maurizio Mencuccini. Australian Government Research Training Program (RTP) Scholarships supported Holly A. A. Beckett and Callum Bryant. The authors thank Tomás Fuenzalida for his contribution to collecting hydraulic vulnerability data. We thank Catherine Bone and Nigel Brothers for exceptional field support and accommodation at the Daintree River, and thank Patrick Meir, Danielle Way, and Matthew Bowes for thoughtful comments on the manuscript. Open access publishing facilitated by Australian National University, as part of the Wiley - Australian National University agreement via the Council of Australian University Librarians.

DATA AVAILABILITY STATEMENT

The data that support the findings of this study are openly accessible at the Australian National University Data Commons. Available from https://doi.org/10.25911/wrg4-wx88.

ORCID

Holly A. A. Beckett http://orcid.org/0000-0001-9593-2430
Callum Bryant http://orcid.org/0000-0002-8035-9157
Teresa Neeman http://orcid.org/0000-0002-7315-3695
Maurizio Mencuccini http://orcid.org/0000-0003-0840-1477
Marilyn C. Ball http://orcid.org/0000-0001-9170-940X

REFERENCES

Adams, H.D., Zeppel, M.J.B., Anderegg, W.R.L., Hartmann, H., Landhäusser, S.M., Tissue, D.T. et al. (2017) A multi-species synthesis of physiological mechanisms in drought-induced tree mortality. *Nature Ecology & Evolution*, 1(9), 1285–1291.

Anderegg, W.R.L., Klein, T., Bartlett, M., Sack, L., Pellegrini, A.F.A., Choat, B. et al. (2016) Meta-analysis reveals that hydraulic traits explain cross-species patterns of drought-induced tree mortality across the globe. *Proceedings of the National Academy of Sciences*, 113(18), 5024–5029.

Arend, M., Link, R.M., Patthey, R., Hoch, G., Schuldt, B. & Kahmen, A. (2021) Rapid hydraulic collapse as cause of drought-induced mortality in conifers. *Proceedings of the National Academy of Sciences*, 118(16), e2025251118. Available from: https://doi.org/10.1073/pnas.2025251118

Baer, A.B., Fickle, J.C., Medina, J., Robles, C., Pratt, R.B. & Jacobsen, A.L. (2021) Xylem biomechanics, water storage, and density within roots and shoots of an angiosperm tree species. *Journal of Experimental Botany*, 72(22), 7984–7997.

Ball, M.C. (1988a) Ecophysiology of mangroves. *Trees*, 2(3), 129–142.

Ball, M.C. (1988b) Salinity tolerance in the mangroves *Aegiceras corniculatum* and *Avicennia marina*. I. Water use in relation to growth, carbon partitioning, and salt balance. *Functional Plant Biology*, 15(3), 447–464.

Barigah, T.S., Bonhomme, M., Lopez, D., Traore, A., Douris, M., Venisse, J.-S. et al. (2013) Modulation of bud survival in *Populus nigra* sprouts in response to water stress-induced embolism. *Tree Physiology*, 33(3), 261–274.

Bartlett, M.K., Klein, T., Jansen, S., Choat, B. & Sack, L. (2016) The correlations and sequence of plant stomatal, hydraulic, and wilting responses to drought. *Proceedings of the National Academy of Sciences*, 113(46), 13098–13103.

Bartlett, M.K., Scoffoni, C. & Sack, L. (2012) The determinants of leaf turgor loss point and prediction of drought tolerance of species and biomes: a global meta-analysis. *Ecology Letters*, 15(5), 393–405.

Bates, D., Mächler, M., Bolker, B. & Walker, S. (2015) Fitting linear mixed-effects models using lme4. *Journal of Statistical Software*, 67, 1–48.

Bazihizina, N., Barrett-Lennard, E.G. & Colmer, T.D. (2012) Plant growth and physiology under heterogeneous salinity. *Plant and Soil*, 354(1), 1–19.

Bazihizina, N., Colmer, T.D. & Barrett-Lennard, E.G. (2009) Response to non-uniform salinity in the root zone of the halophyte *Atriplex nummularia*: growth, photosynthesis, water relations and tissue ion concentrations. *Annals of Botany*, 104(4), 737–745.

Beckett, H.A.A., Neeman, T., Fuenzalida, T.I., Bryant, C., Latorre, S.C., Ovington, L.I. et al. (2023) Ghosts of dry seasons past: legacy of severe drought enhances mangrove salinity tolerance through coordinated cellular osmotic and elastic adjustments. *Plant, cell & environment*, 46(7), 2031–2045.

Beikircher, B. & Mayr, S. (2009) Intraspecific differences in drought tolerance and acclimation in hydraulics of *Ligustrum vulgare* and *Viburnum lantana*. *Tree Physiology*, 29(6), 765–775.

Bittencourt, P.R.L., Oliveira, R.S., da Costa, A.C.L., Giles, A.L., Coughlin, I., Costa, P.B. et al. (2020) Amazonia trees have limited capacity to acclimate plant hydraulic properties in response to long-term drought. *Global Change Biology*, 26(6), 3569–3584.

Brodersen, C.R., McElrone, A.J., Choat, B., Matthews, M.A. & Shackel, K.A. (2010) The dynamics of embolism repair in xylem: in vivo visualizations using high-resolution computed tomography. *Plant Physiology*, 154(3), 1088–1095.

Bryant, C., Fuenzalida, T.I., Brothers, N., Mencuccini, M., Sack, L., Binks, O. et al. (2021) Shifting access to pools of shoot water sustains gas exchange and increases stem hydraulic safety during seasonal atmospheric drought. *Plant, Cell & Environment*, 44(9), 2898–2911.

Cai, J., Li, S., Zhang, H., Zhang, S. & Tyree, M.T. (2014) Recalcitrant vulnerability curves: methods of analysis and the concept of fibre bridges for enhanced cavitation resistance. *Plant, Cell & Environment*, 37(1), 35–44.

Chapotin, S.M., Razanameharizaka, J.H. & Holbrook, N.M. (2006) A biomechanical perspective on the role of large stem volume and high water content in baobab trees (Adansonia spp.; Bombacaceae). *American Journal of Botany*, 93(9), 1251–1264.

Cheung, Y.N.S., Tyree, M.T. & Dainty, J. (1975) Water relations parameters on single leaves obtained in a pressure bomb and some ecological interpretations. *Canadian Journal of Botany*, 53(13), 1342–1346.

Choat, B., Cobb, A.R. & Jansen, S. (2008) Structure and function of bordered pits: new discoveries and impacts on whole-plant hydraulic function. *New Phytologist*, 177(3), 608–626.

Choat, B., Jansen, S., Brodribb, T.J., Cochard, H., Delzon, S., Bhaskar, R. et al. (2012) Global convergence in the vulnerability of forests to drought. *Nature*, 491(7426), 752–755.

Clough, B. (1984) Growth and salt balance of the mangroves *Avicennia marina* (Forsk.) Vierh. and Rhizophora stylosa Griff. in relation to salinity. *Functional Plant Biology*, 11(5), 419–430.

Coopman, R.E., Nguyen, H.T., Mencuccini, M., Oliveira, R.S., Sack, L., Lovelock, C.E. et al. (2021) Harvesting water from unsaturated atmospheres: deliquescence of salt secreted onto leaf surfaces drives reverse sap flow in a dominant arid climate mangrove, *Avicennia marina*. *New Phytologist*, 231(4), 1401–1414.

Domec, J.-C. & Gartner, B.L. (2001) Cavitation and water storage capacity in bole xylem segments of mature and young Douglas-fir trees. *Trees*, 15(4), 204–214.

Duke, N.C., Kovacs, J.M., Griffiths, A.D., Preece, L., Hill, D.J.E., van Oosterzee, P. et al. (2017) Large-scale dieback of mangroves in Australia. *Marine and Freshwater Research*, 68(10), 1816–1829.

Duursma, R. & Choat, B. (2017) fitplc—an R package to fit hydraulic vulnerability curves. *Journal of Plant Hydraulics*, 4(0), e002.

Epila, J., De Baerdemaeker, N.J.F., Vergeynst, L.L., Maes, W.H., Beeckman, H. & Steppe, K. (2017) Capacitive water release and internal leaf water relocation delay drought-induced cavitation in African *Maesopsis eminii*. *Tree Physiology*, 37(4), 481–490.

Feng, F., Wagner, Y., Klein, T. & Hochberg, U. (2023) Xylem resistance to cavitation increases during summer in *Pinus halepensis*. *Plant, Cell & Environment*, 46(6), 1849–1859.

Fricke, W. (2017) Turgor Pressure. In: *eLS*. 1–6.

Gessler, A. (2021) Water transport in trees—the importance of radial and circumferential transport. *Tree Physiology*, 41, 2245–2247.

Gleason, S.M., Blackman, C.J., Cook, A.M., Laws, C.A. & Westoby, M. (2014) Whole-plant capacitance, embolism resistance and slow transpiration rates all contribute to longer desiccation times in woody angiosperms from arid and wet habitats. *Tree Physiology*, 34(3), 275–284.

Goldstein, G., Andrade, J.L., Meinzer, F.C., Holbrook, N.M., Cavelier, J., Jackson, P. et al. (1998) Stem water storage and diurnal patterns of water use in tropical forest canopy trees. *Plant, Cell & Environment*, 21(4), 397–406.

Guadagno, C.R., Ewers, B.E., Speckman, H.N., Aston, T.L., Huhn, B.J., DeVore, S.B. et al. (2017) Dead or alive? Using membrane failure and chlorophyll a fluorescence to predict plant mortality from drought. *Plant Physiology*, 175(1), 223–234.

Guillemot, J., Martin-StPaul, N.K., Bulascoschi, L., Poorter, L., Morin, X., Pinho, B.X. et al. (2022) Small and slow is safe: on the drought tolerance of tropical tree species. *Global Change Biology*, 28(8), 2622–2638.

Harris, R.M.B., Beaumont, L.J., Vance, T.R., Tozer, C.R., Remenyi, T.A., Perkins-Kirkpatrick, S.E. et al. (2018) Biological responses to the press and pulse of climate trends and extreme events. *Nature Climate Change*, 8(7), 579–587.

Herbette, S., Bouchet, B., Brunel, N., Bonnin, E., Cochard, H. & Guillon, F. (2015) Immunolabelling of intervessel pits for polysaccharides and lignin helps in understanding their hydraulic properties in *Populus tremula* × alba. *Annals of Botany*, 115(2), 187–199.

Hochberg, U., Albuquerque, C., Rachmilevitch, S., Cochard, H., David-Schwartz, R., Brodersen, C.R. et al. (2016) Grapevine petioles are more sensitive to drought induced embolism than stems: evidence from in vivo MRI and microcomputed tomography observations of hydraulic vulnerability segmentation. *Plant, Cell & Environment*, 39(9), 1886–1894.

Holbrook, N.M. & Sinclair, T.R. (1992) Water balance in the arborescent palm, *Sabal palmetto*. II. Transpiration and stem water storage. *Plant, Cell & Environment*, 15(4), 401–409.

IPCC. (2022) Climate change 2022: i*mpacts, adaptation, and vulnerability. contribution of working group ii to the sixth assessment report of the intergovernmental panel on climate change*. Cambridge, UK and New York, NY, USA: Cambridge University Press.

Jacobsen, A.L., Pratt, R.B., Davis, S.D. & Tobin, M.F. (2014) Geographic and seasonal variation in chaparral vulnerability to cavitation. *Madroño*, 61(4), 317–327.

Jacobsen, A.L., Pratt, R.B., Davis, S.D. & Ewers, F.W. (2007) Cavitation resistance and seasonal hydraulics differ among three arid Californian plant communities. *Plant, Cell & Environment*, 30(12), 1599–1609.

Jansen, S., Bittencourt, P., Pereira, L., Schenk, H.J. & Kunert, N. (2022) A crucial phase in plants - it's a gas, gas, gas! *New Phytologist*, 233(4), 1556–1559.

Jansen, S., Choat, B. & Pletsers, A. (2009) Morphological variation of intervessel pit membranes and implications to xylem function in angiosperms. *American Journal of Botany*, 96(2), 409–419.

Knipfer, T., Reyes, C., Earles, J.M., Berry, Z.C., Johnson, D.M., Brodersen, C.R. et al. (2019) Spatiotemporal coupling of vessel cavitation and discharge of stored xylem water in a tree sapling. *Plant Physiology*, 179(4), 1658–1668.

Kolb, K.J. & Sperry, J.S. (1999) Transport constraints on water use by the Great Basin shrub, *Artemisia tridentata*. *Plant, Cell & Environment*, 22, 925–935.

Kuznetsova, A., Brockhoff, P.B. & Christensen, R.H.B. (2017) lmerTest package: tests in linear mixed effects models. *Journal of Statistical Software*, 82(13), 1–26.

Ladjal, M., Huc, R. & Ducrey, M. (2005) Drought effects on hydraulic conductivity and xylem vulnerability to embolism in diverse species and provenances of Mediterranean cedars. *Tree Physiology*, 25(9), 1109–1117.

Lamacque, L., Charrier, G., Farnese, F.S., Lemaire, B., Améglio, T. & Herbette, S. (2020) Drought-induced mortality: branch diameter variation reveals a point of no recovery in lavender species. *Plant Physiology*, 183(4), 1638–1649.

Lambers, H. & Oliveira, R.S. (2019) Plant water relations. In: Lambers, H. & Oliveira, R.S. (Eds.) *Plant physiological ecology*. New York, NY: Springer International Publishing, pp. 187–263.

Lamy, J.B., Delzon, S., Bouche, P.S., Alia, R., Vendramin, G.G., Cochard, H. et al. (2014) Limited genetic variability and phenotypic plasticity detected for cavitation resistance in a Mediterranean pine. *New Phytologist*, 201(3), 874–886.

Lenth, R.V. (2020) *emmeans: estimated marginal means, aka least-squares means*. https://CRAN.R-project.org/package=emmeans

Loustau, D., Berbigier, P., Roumagnac, P., Arruda-Pacheco, C., David, J.S., Ferreira, M.I. et al. (1996) Transpiration of a 64-year-old maritime pine stand in Portugal: 1. Seasonal course of water flux through maritime pine. *Oecologia*, 107(1), 33–42.

Mantova, M., Herbette, S., Cochard, H. & Torres-Ruiz, J.M. (2022) Hydraulic failure and tree mortality: from correlation to causation. *Trends in Plant Science*, 27(4), 335–345.

Martinez-Vilalta, J., Anderegg, W.R.L., Sapes, G. & Sala, A. (2019) Greater focus on water pools may improve our ability to understand and anticipate drought-induced mortality in plants. *New Phytologist*, 223(1), 22–32.

Martínez-Vilalta, J., Cochard, H., Mencuccini, M., Sterck, F., Herrero, A., Korhonen, J.F.J. et al. (2009) Hydraulic adjustment of Scots pine across Europe. *New Phytologist*, 184(2), 353–364.

Martin-StPaul, N., Delzon, S. & Cochard, H. (2017) Plant resistance to drought depends on timely stomatal closure. *Ecology Letters*, 20(11), 1437–1447.

McDowell, N.G., Ball, M., Bond-Lamberty, B., Kirwan, M.L., Krauss, K.W., Megonigal, J.P. et al. (2022a) Processes and mechanisms of coastal woody-plant mortality. *Global Change Biology*, 28(20), 5881–5900.

McDowell, N.G., Sapes, G., Pivovaroff, A., Adams, H.D., Allen, C.D. et al. (2022b) Mechanisms of woody-plant mortality under rising drought, CO2 and vapour pressure deficit. *Nature Reviews Earth & Environment*, 3(5), 294–308.

Meinzer, F.C., James, S.A., Goldstein, G. & Woodruff, D. (2003) Whole-tree water transport scales with sapwood capacitance in tropical forest canopy trees. *Plant, Cell & Environment*, 26(7), 1147–1155.

Meinzer, F.C., Johnson, D.M., Lachenbruch, B., McCulloh, K.A. & Woodruff, D.R. (2009) Xylem hydraulic safety margins in woody plants: coordination of stomatal control of xylem tension with hydraulic capacitance. *Functional Ecology*, 23(5), 922–930.

Meinzer, F.C., Woodruff, D.R., Domec, J.-C., Goldstein, G., Campanello, P.I., Gatti, M.G. et al. (2008) Coordination of leaf and stem water transport properties in tropical forest trees. *Oecologia*, 156(1), 31–41.

Mencuccini, M. & Comstock, J. (1997) Vulnerability to cavitation in populations of two desert species, Hymenoclea salsola and *Ambrosia dumosa*, from different climatic regions. *Journal of Experimental Botany*, 48(6), 1323–1334.

Naidoo, G. (1985) Effects of waterlogging and salinity on plant-water relations and on the accumulation of solutes in three mangrove species. *Aquatic Botany*, 22(2), 133–143.

Naidoo, G., Hiralal, O. & Naidoo, Y. (2011) Hypersalinity effects on leaf ultrastructure and physiology in the mangrove *Avicennia marina*. *Flora - Morphology, Distribution, Functional Ecology of Plants*, 206(9), 814–820.

Nardini, A., Lo Gullo, M.A. & Salleo, S. (2011) Refilling embolized xylem conduits: is it a matter of phloem unloading? *Plant Science*, 180(4), 604–611.

Nguyen, H.T., Meir, P., Sack, L., Evans, J.R., Oliveira, R.S. & Ball, M.C. (2017a) Leaf water storage increases with salinity and aridity in the mangrove *Avicennia marina*: integration of leaf structure, osmotic adjustment and access to multiple water sources. *Plant, Cell & Environment*, 40(8), 1576–1591.

Nguyen, H.T., Meir, P., Wolfe, J., Mencuccini, M. & Ball, M.C. (2017b) Plumbing the depths: extracellular water storage in specialized leaf structures and its functional expression in a three-domain pressure - volume relationship. *Plant, Cell & Environment*, 40(7), 1021–1038.

Ogle, K., Barber, J.J., Willson, C. & Thompson, B. (2009) Hierarchical statistical modeling of xylem vulnerability to cavitation. *New Phytologist*, 182(2), 541–554.

Oliva Carrasco, L., Bucci, S.J., Di Francescantonio, D., Lezcano, O.A., Campanello, P.I., Scholz, F.G. et al. (2015) Water storage dynamics in the main stem of subtropical tree species differing in wood density, growth rate and life history traits. *Tree Physiology*, 35(4), 354–365.

Oliveira, R.S., Christoffersen, B.O., de V. Barros, F., Teodoro, G.S., Bittencourt, P., Brum-Jr, M.M. et al. (2014) Changing precipitation regimes and the water and carbon economies of trees. *Theoretical and Experimental Plant Physiology*, 26(1), 65–82.

Panshin, A.J. & De Zeeuw, C. (1980) *Textbook of wood technology: structure, identification, properties, and uses of the commercial woods of the United States and Canada*. New York: McGraw-Hill.

Pereira, L., Bittencourt, P.R.L., Oliveira, R.S., Junior, M.B.M., Barros, F.V., Ribeiro, R.V. et al. (2016) Plant pneumatics: stem air flow is related to embolism - new perspectives on methods in plant hydraulics. *New Phytologist*, 211(1), 357–370.

Pereira, L., Domingues-Junior, A.P., Jansen, S., Choat, B. & Mazzafera, P. (2018a) Is embolism resistance in plant xylem associated with quantity and characteristics of lignin? *Trees*, 32(2), 349–358.

Pereira, L., Flores-Borges, D.N.A., Bittencourt, P.R.L., Mayer, J.L.S., Kiyota, E., Araújo, P. et al. (2018b) Infrared nanospectroscopy reveals the chemical nature of pit membranes in water-conducting cells of the plant xylem. *Plant Physiology*, 177(4), 1629–1638.

Peters, R.L., Steppe, K., Cuny, H.E., De Pauw, D.J.W., Frank, D.C., Schaub, M. et al. (2021) Turgor - a limiting factor for radial growth in mature conifers along an elevational gradient. *New Phytologist*, 229(1), 213–229.

Pfautsch, S., Renard, J., Tjoelker, M.G. & Salih, A. (2015) Phloem as capacitor: radial transfer of water into xylem of tree stems occurs via symplastic transport in ray parenchyma. *Plant Physiology*, 167(3), 963–971.

Powers, J.S., Vargas, G., Brodribb, T.J., Schwartz, N.B., Pérez-Aviles, D., Smith-Martin, C.M. et al. (2020) A catastrophic tropical drought kills hydraulically vulnerable tree species. *Global Change Biology*, 26(5), 3122–3133.

Preisler, Y., Hölttä, T., Grünzweig, J.M., Oz, I., Tatarinov, F., Ruehr, N.K. et al. (2022) The importance of tree internal water storage under drought conditions. *Tree Physiology*, 42(4), 771–783.

Preisler, Y., Tatarinov, F., Grünzweig, J.M. & Yakir, D. (2021) Seeking the "point of no return" in the sequence of events leading to mortality of mature trees. *Plant, Cell & Environment*, 44(5), 1315–1328.

R Core Team. (2023) *R: a language and environment for statistical computing*. R Foundation for Statistical Computing. https://www.R-project.org/

Reef, R., Markham, H.L., Santini, N.S. & Lovelock, C.E. (2015) The response of the mangrove *Avicennia marina* to heterogeneous salinity measured using a split-root approach. *Plant and Soil*, 393(1), 297–305.

Robert, E.M.R., Koedam, N., Beeckman, H. & Schmitz, N. (2009) A safe hydraulic architecture as wood anatomical explanation for the difference in distribution of the mangroves Avicennia and Rhizophora. *Functional Ecology*, 23(4), 649–657.

Rodriguez-Dominguez, C.M., Carins Murphy, M.R., Lucani, C. & Brodribb, T.J. (2018) Mapping xylem failure in disparate organs of whole plants reveals extreme resistance in olive roots. *New Phytologist*, 218(3), 1025–1035.

Salleo, S., Trifilò, P., Esposito, S., Nardini, A. & Lo Gullo, M.A. (2009) Starch-to-sugar conversion in wood parenchyma of field-growing *Laurus nobilis* plants: a component of the signal pathway for embolism repair? *Functional Plant Biology*, 36(9), 815–825.

Sapes, G. & Sala, A. (2021) Relative water content consistently predicts drought mortality risk in seedling populations with different morphology, physiology and times to death. *Plant, Cell & Environment*, 44(10), 3322–3335.

Schenk, H.J., Espino, S., Romo, D.M., Nima, N., Do, A.Y.T., Michaud, J.M. et al. (2017) Xylem surfactants introduce a new element to the cohesion-tension theory. *Plant Physiology*, 173(2), 1177–1196.

Schindelin, J., Arganda-Carreras, I., Frise, E., Kaynig, V., Longair, M., Pietzsch, T. et al. (2012) Fiji: an open-source platform for biological-image analysis. *Nature Methods*, 9(7), 676–682.

Scholander, P.F., Bradstreet, E.D., Hammel, H.T. & Hemmingsen, E.A. (1966) Sap concentrations in halophytes and some other plants. *Plant Physiology*, 41(3), 529–532.

Scholander, P.F., Hammel, H.T., Hemmingsen, E.A. & Bradstreet, E.D. (1964) Hydrostatic pressure and osmotic potential in leaves of mangroves and some other plants. *Proceedings of the National Academy of Sciences*, 52(1), 119–125.

Scholz, F.G., Bucci, S.J., Goldstein, G., Meinzer, F.C., Franco, A.C. & Miralles-Wilhelm, F. (2007) Biophysical properties and functional significance of stem water storage tissues in Neotropical savanna trees. *Plant, Cell & Environment*, 30(2), 236–248.

Scholz, F.G., Phillips, N.G., Bucci, S.J., Meinzer, F.C. & Goldstein, G. (2011) Hydraulic capacitance: biophysics and functional significance of internal water sources in relation to tree size. In: Meinzer, F.C., Lachenbruch, B. & Dawson, T.E. (Eds.) *Size- and age-related changes in tree structure and function*. Netherlands: Springer, pp. 341–361.

Schuldt, B., Knutzen, F., Delzon, S., Jansen, S., Müller-Haubold, H., Burlett, R. et al. (2016) How adaptable is the hydraulic system of European beech in the face of climate change-related precipitation reduction? *New Phytologist*, 210(2), 443–458.

Sergent, A.S., Varela, S.A., Barigah, T.S., Badel, E., Cochard, H., Dalla-Salda, G. et al. (2020) A comparison of five methods to assess embolism resistance in trees. *Forest Ecology and Management*, 468, 118175.

Sevanto, S., McDowell, N.G., Dickman, L.T., Pangle, R. & Pockman, W.T. (2014) How do trees die? A test of the hydraulic failure and carbon starvation hypotheses. *Plant, Cell & Environment*, 37(1), 153–161.

Steppe, K. & Lemeur, R. (2004) An experimental system for analysis of the dynamic sap-flow characteristics in young trees: results of a beech tree. *Functional Plant Biology*, 31(1), 83–92.

Stiller, V. (2009) Soil salinity and drought alter wood density and vulnerability to xylem cavitation of baldcypress (*Taxodium distichum* (L.) Rich.) seedlings. *Environmental and Experimental Botany*, 67(1), 164–171.

Stuart, S.A., Choat, B., Martin, K.C., Holbrook, N.M. & Ball, M.C. (2007) The role of freezing in setting the latitudinal limits of mangrove forests. *New Phytologist*, 173(3), 576–583.

Treydte, K., Lehmann, M.M., Wyczesany, T. & Pfautsch, S. (2021) Radial and axial water movement in adult trees recorded by stable isotope tracing. *Tree Physiology*, 41(12), 2248–2261.

Trueba, S., Pouteau, R., Lens, F., Feild, T.S., Isnard, S., Olson, M.E. et al. (2017) Vulnerability to xylem embolism as a major correlate of the environmental distribution of rain forest species on a tropical island. *Plant, Cell & Environment*, 40(2), 277–289.

Tyree, M.T. & Hammel, H.T. (1972) The measurement of the turgor pressure and the water relations of plants by the pressure-bomb technique. *Journal of Experimental Botany*, 23(1), 267–282.

Waring, R.H., Whitehead, D. & Jarvis, P.G. (2006) The contribution of stored water to transpiration in Scots pine. *Plant, Cell & Environment*, 2, 309–317.

Warton, D.I., Duursma, R.A., Falster, D.S. & Taskinen, S. (2012) smatr 3—an R package for estimation and inference about allometric lines. *Methods in Ecology and Evolution*, 3(2), 257–259.

Wickham, H. (2016) *ggplot2: elegant graphics for data analysis*. New York: Springer-Verlag. https://ggplot2.tidyverse.org

Yazaki, K., Levia, D.F., Takenouchi, A., Watanabe, M., Kabeya, D., Miki, N.H. et al. (2020) Imperforate tracheary elements and vessels alleviate xylem tension under severe dehydration: insights from water release curves for excised twigs of three tree species. *American Journal of Botany*, 107(8), 1122–1135.

Zhang, Y., Lamarque, L.J., Torres-Ruiz, J.M., Schuldt, B., Karimi, Z., Li, S. et al. (2018) Testing the plant pneumatic method to estimate xylem embolism resistance in stems of temperate trees. *Tree Physiology*, 38(7), 1016–1025.

Zimmermann, M.H. (1983) The hydraulic architecture of plants. In: Zimmermann, M.H. (Ed.) *Xylem structure and the ascent of sap*. Heidelberg: Springer Berlin, pp. 66–82.

Zweifel, R., Drew, D.M., Schweingruber, F. & Downes, G.M. (2014) Xylem as the main origin of stem radius changes in Eucalyptus. *Functional Plant Biology*, 41(5), 520–534.

SUPPORTING INFORMATION

Additional supporting information can be found online in the Supporting Information section at the end of this article.

How to cite this article: Beckett, H. A. A., Bryant, C., Neeman, T., Mencuccini, M. & Ball, M. C. (2024) Plasticity in branch water relations and stem hydraulic vulnerability enhances hydraulic safety in mangroves growing along a salinity gradient. *Plant, Cell & Environment*, 47, 854–870. https://doi.org/10.1111/pce.14764